

# Impact of Choline Chloride/1,4-Butanediol Deep Eutectic Solvent on Tamarind Seed Polysaccharide-Based Polymer Electrolyte Films

Muhammad Hanif Mohd Fauzee<sup>1</sup>, Nurul Farah Atieqah Suddin<sup>1</sup>, Nabilah Akemal Muhd Zailani<sup>1,\*</sup>, Khuzaimah Nazir<sup>1</sup>, Sharifah Nafisah Syed Ismail<sup>1</sup>, Nurul Aizan Mohd Zaini<sup>1</sup>, Solhan Yahya<sup>1</sup> and Famiza Abdul Latif<sup>2</sup>

<sup>1</sup>Faculty of Applied Sciences, Universiti Teknologi MARA, Cawangan Perlis, Kampus Arau, 02600 Arau, Perlis, Malaysia

<sup>2</sup>Faculty of Applied Sciences, Universiti Teknologi MARA, 40450 Shah Alam, Selangor, Malaysia

\*Corresponding author (e-mail: nabilahakemal@uitm.edu.my)

The presence of hydroxyl groups in polysaccharides results in brittle electrolyte films with poor ionic conductivity. The incorporation of traditional plasticizers like ethylene carbonate (EC) and propylene carbonate (PC) had effectively addressed the brittleness problem, but these plasticizers pose health risks. Thus, in this study, different weight percentages (%) (i.e., 0.2, 0.3, 0.4, 0.5, and 0.6 wt%) of choline chloride:1,4-butanediol (ChCl:1,4-BD), deep eutectic solvent (DES) with lower toxicity were incorporated into the tamarind seed polysaccharide (TSP) matrix. Then, the structural, electrical, morphological, and mechanical properties of the films obtained were evaluated. The polymer electrolyte films were prepared using the solution casting technique and a fixed amount of lithium triflate (LiTf) was added as the additional conducting species. A flexible and free-standing film of TSP-based electrolyte at the highest ionic conductivity of  $2.30 \times 10^{-4} \text{ S cm}^{-1}$  was successfully obtained with the addition of 0.4 wt% of DES (TSPL 0.4). This was probably due to the successful prevention of hydrogen bonding as DES occupied the spaces between TSP chains. This could be further supported by the TSP-DES, TSP-LiTf, and salt-DES interactions as confirmed from Fourier transform infrared spectroscopy (FTIR) analyses. The smooth surface with no agglomeration due to salt and DES particles was observed for the optical micrograph of TSPL 0.4. This is due to the salt-DES interaction, which also contributes to the enhancement of the ionic conductivity of TSPL 0.4. The tensile test demonstrates the maximum tensile strain of 50.00% for TSPL 0.4, indicating the highest flexibility of the sample.

**Keywords:** Tamarind seed polysaccharide; deep eutectic solvent; flexible film; lithium-ion batteries

*Received: January 2024; Accepted: March 2024*

Lithium-ion batteries, extensively researched for their energy storage capabilities, offer numerous benefits such as high ionic conductivity, cost-effectiveness, efficient material usage, and established manufacturing methods. Despite these advantages, the conventional liquid electrolytes commonly used in lithium-ion batteries pose safety risks due to their inherent flammability and volatility, leading to issues like leakage, corrosion, and explosion [1]. As a result, polymer electrolytes are employed as a safer alternative to mitigate these issues.

Polymer electrolytes typically form through the dissolution of salt in the polymer host, which could be either a natural or synthetic polymer. Natural polymers can be obtained from nature, while synthetic polymers are man-made. Natural polymers, primarily composed of polysaccharides, are known to be safe and less harmful. Meanwhile, synthetic polymers, which are commonly utilized in medical devices, are known for their versatility [2]. Natural polymers such

as starch, cellulose, chitosan, carboxymethyl cellulose, and carrageenan have been investigated in recent studies due to their low cost and accessibility [3-4].

Tamarind seed polysaccharide (TSP) is one of the natural polymers obtained from agricultural waste. TSP owns exceptional qualities like a good gelling agent and an easy capacity for film formation. TSP can be utilized as polymer electrolytes due to the presence of oxygen atoms for coordinating sites. However, the presence of hydroxyl groups in TSP initiates the formation of hydrogen bonding between the chains, hence causing the brittleness of the electrolyte films. The brittle films will negatively impact the electrode-electrolyte interaction, reducing ionic conductivity and the efficiency of energy storage devices. To address this issue, plasticizers like phthalic acid esters, dioctyl phthalate (DOP), ethylene carbonate (EC), and propylene carbonate (PC) are added to enhance the flexibility of the films by increasing free volume between polymer chains [5-6]. Despite their effectiveness, these

plasticizers, derived from non-renewable sources, raise environmental concerns due to their resistance to solar radiation and microbial degradation [7]. Additionally, they are highly toxic and contribute to reproductive and developmental issues [8-9].

The environmentally friendly deep eutectic solvent (DES) is the best alternative to the conventional plasticizers, as it has lower toxicity and is more biodegradable [10]. DES consists of two or three substances acting as hydrogen bond donors (HBD) and hydrogen bond acceptors (HBA), which associate to form eutectic mixture with lower melting point than its constituents [11]. Thus, in this study, flexible and free-standing films were prepared by the addition of choline chloride/1, 4-butanediol (ChCl: 1,4-BD) DES into the TSP-based polymer electrolyte system. ChCl: 1,4-BD was chosen as it is included in Type III DES that requires low-cost preparation and presents low eco-toxicity [12]. Lithium triflate (LiTf) was also added to the system at a fixed amount to provide the additional conducting species. The bulky structure of DES was expected to occupy the space between the polysaccharide chains, hence disrupting the hydrogen bonding. To determine the optimum amount of DES for this system, the effect of the various weight percentages of ChCl: 1,4-BD on the structural, electrical, morphological, and mechanical properties of the TSP-based electrolyte system was specifically studied.

## EXPERIMENTAL

### Chemicals and Materials

TSP and LiTf (Purity: 99.995%) were purchased from Tokyo Chemical Industry, Japan and Sigma-Aldrich, respectively. Meanwhile, the DES with 1:3 mole ratio of ChCl:1,4-BD was previously prepared in the preliminary study. None of the compounds were purified before usage.

### Preparation of Plasticized TSP-based Electrolyte Films

The film samples were prepared using solvent casting technique adapted from the study by Sampath Kumar et al. [3]. A total of 1.0000 g of TSP was dissolved in 100 mL of hot double-distilled water at 80°C on magnetic stirrer at 600 rpm for 10 minutes until dissolution. Meanwhile, 0.4500 g of LiTf was dissolved

in distilled water by stirring continuously for a few hours at room temperature. Then, the host polymer and ionic salt were combined and stirred using magnetic stirrer at room temperature to achieve a homogeneous solution mix. The TSP-LiTf electrolyte solution was added with 0.2, 0.3, 0.4, 0.5, and 0.6 wt% of DES as plasticizer, as shown in Table 1. The mixtures were stirred until a homogenous solution was achieved. The obtained solutions were then cast onto petri dishes and dried inside a hot air oven at 60°C until the formation of the films. Blank TSP and TSP/LiTf films were prepared as controls.

## Characterization Methods

### Fourier Transform Infrared Spectroscopy (FTIR)

FTIR (Thermo Fisher Scientific Nicolet iS 10) with Attenuated Total Reflectance (ATR) was used to obtain the spectra of the film samples at room temperature. The FTIR study aimed to determine the interactions between TSP, LiTf, and DES. The samples were put directly onto the crystal before being subjected to transmittance mode measurements over the frequency range of 4000 cm<sup>-1</sup> – 600 cm<sup>-1</sup> with resolutions of 2 cm<sup>-1</sup> and 16 scans.

### Electrochemical Impedance Spectroscopy (EIS)

EIS (HIOKI 35232-01 LCR) was used to measure the ionic conductivity of the plasticized TSP-based polymer electrolyte system. At room temperature, the impedance of the films was measured at frequencies between 100 Hz – 1 MHz. The measurement was taken when the polymer electrolyte film is positioned between two stainless steel blocking electrodes. A micrometer screw gauge was used to measure the thickness of the films prior to measurement. In three distinct regions of the films, the impedance was measured, and the average ionic conductivity of each sample was evaluated using Equation (1).

$$\sigma = \frac{l}{R_b \cdot A} \quad (1)$$

Where,  $R_b$  is the bulk resistance ( $\Omega$ ),  $l$  is the thickness of the film (cm), and  $A$  is the effective contact area of the electrode and the electrolyte (cm<sup>2</sup>).

**Table 1.** Compositions of plasticized TSP-based polymer electrolyte system.

Weight of TSP (g)	Weight of LiTf (g)	Weight percentage of DES (wt%)	Weight of DES (g)	Designation
1.0000	0.4500	0.0	0.0000	TSP
		0.0	0.0000	TSPL
		0.2	0.0029	TSPL 0.2
		0.3	0.0044	TSPL 0.3
		0.4	0.0058	TSPL 0.4
		0.5	0.0073	TSPL 0.5
		0.6	0.0088	TSPL 0.6

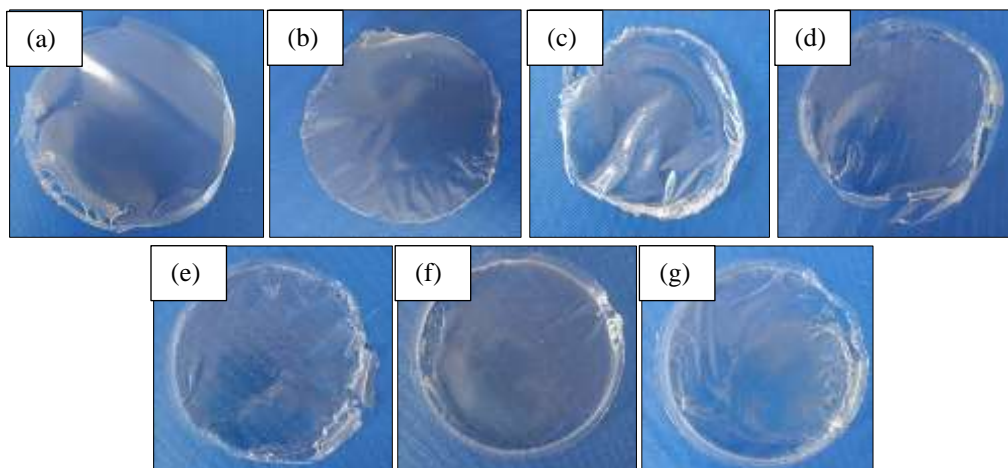


**Figure 1.** Films of (a) pure TSP, (b) TSPL, (c) TSPL 0.2, (d) TSPL 0.3, (e) TSPL 0.4, (f) TSPL 0.5, and (g) TSPL 0.6.

### Optical Microscopy (OM)

The morphology of the plasticized TSP-based electrolyte films was viewed using optical microscope (Olympus CX31 Microscope). 10x magnification was used to examine the materials.

### Universal Testing Machine (UTM)

The Instron Universal Testing Instrument (3365, Instron USA) was used to assess the mechanical properties of the film samples (i.e., tensile strain, tensile stress, and Young's modulus). Each sample was cut into 1 cm x 7.0 cm pieces and tested at 25cm/min cross-speed according to ASTM D882. Three replicates were performed for each sample formulation.

## RESULTS AND DISCUSSION

### Formation of Plasticized TSP-based Electrolyte Films

The brittle structure of pure TSP and TSPL films are depicted in Figures 1 (a)-(b). This happens because of the polysaccharide's OH groups, which tend to form hydrogen bonds between the polymer chains. The same observation was reported by Maithilee et al. [13]. Figures 1 (c)-(g) show flexible and free-standing films after the addition of various amounts of DES. This might be due to the bulky structure of DES that occupies the spaces between the polysaccharide chains, hence disrupting the hydrogen bonding. This is consistent with the findings of Nardecchia et al. [14], who reported that the addition of DES encouraged the stabilization of polypeptides towards its collapsed state.

### FTIR Studies

The FTIR spectra of TSP, TSPL and TSPL 0.2-0.6 are depicted in Figure 2. The band assignments and the shifts in the vibrational peaks of the prepared polymer electrolytes are listed in Table 2. From the FTIR spectra, pure TSP showed vibrational bands at  $3340\text{ cm}^{-1}$ ,  $2924\text{ cm}^{-1}$ ,  $1636\text{ cm}^{-1}$ ,  $1361\text{ cm}^{-1}$ ,  $1038\text{ cm}^{-1}$ , and  $942\text{ cm}^{-1}$ , which represent O-H stretching,  $\text{CH}_2$  stretching, C=C stretching,  $\text{CH}_2$  bending, C-O-C stretching, and C-H bending, respectively. The same position of peaks was also reported by Premalatha et al. [4].

When LiTf was added to the TSP matrix, the peaks representing LiTf were observed at  $1265$  and  $1182\text{ cm}^{-1}$  for  $\text{SO}_3$  stretching and of  $\text{CF}_3$  stretching, respectively. This indicates the successful incorporation of LiTf into the TSP matrix. Due to that, the downshifting of the wavenumber was also observed for O-H stretching from  $3340$  to  $3375\text{ cm}^{-1}$ , along with the increase in peak intensity. There also occurred an upshifting of the wavenumber in C-O-C stretching peak from  $1038$  to  $1022\text{ cm}^{-1}$ , along with the reduce in peak intensity. These observations confirm the interaction between oxygen atoms in the TSP and the  $\text{Li}^+$  of LiTf. The same observation was also reported by Sampath Kumar et al. [3], who studied on TSP-LiTf interaction.

After the incorporation of DES, the peak for DES was observed at  $1074\text{ cm}^{-1}$ , representing C-N stretching. This indicates the successful incorporation of DES into the TSP matrix. This is supported by the study done by Latif et al. [15] who studied on the effect of ChCl-based DES on the properties of PMMA films. The wavenumber of O-H stretching shifted from  $3375\text{ cm}^{-1}$  to  $3394$ ,  $3391$ ,  $3381$ ,  $3371$ , and  $3371\text{ cm}^{-1}$  when 0.2, 0.3, 0.4, 0.5, and 0.6 wt% of DES were added, respectively. Meanwhile, for C-O-C stretching, the wavenumber shifted from  $1022\text{ cm}^{-1}$  to  $1026$ ,  $1027$ ,  $1025$ ,  $1027$ , and  $1027\text{ cm}^{-1}$  when 0.2, 0.3, 0.4, 0.5, and 0.6 wt% of DES were added, respectively.

Thus, this confirms the interaction between oxygen atoms in the TSP with the choline cation of DES. For  $\text{SO}_3$  and  $\text{CF}_3$  stretching peaks of salt, the decrease in the wavenumbers from  $1265\text{ cm}^{-1}$  to  $1248$ ,  $1249$ ,  $1249$ ,  $1250$ , and  $1251\text{ cm}^{-1}$  and from  $1182\text{ cm}^{-1}$  to  $1172$ ,  $1171$ ,  $1168$ ,  $1168$ , and  $1167\text{ cm}^{-1}$  after addition of 0.2, 0.3, 0.4, 0.5 and 0.6 wt% of DES, respectively, were observed. This indicates the occurrence of salt-DES interaction.

### Conductivity Studies

Figure 3 shows the Cole-Cole plots for pure TSP, TSPL, and TSPL 0.2 – 0.6. A depressed semicircle

was observed at the low frequency region for TSP and TSPL, indicating the bulk resistance of the polymer electrolyte [16]. Meanwhile, a spike was observed at the high frequency region for TSPL and TSPL 0.2 – 0.6, ascribing to the effect of blocking resistance due to the electrode-electrolyte interface [16]. From the Cole-Cole plots, the value of bulk resistance ( $R_b$ ) was determined, and the ionic conductivity was calculated using Equation (1). Table 3 lists the ionic conductivity values for all the samples, while Figure 4 illustrates the plot of ionic conductivity versus weight percentage of DES.

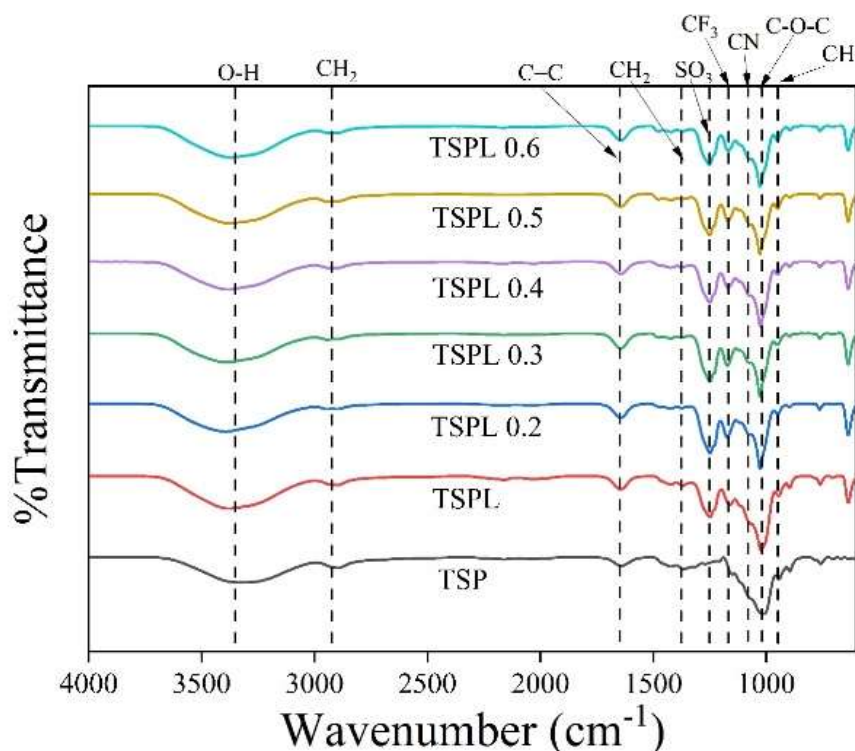
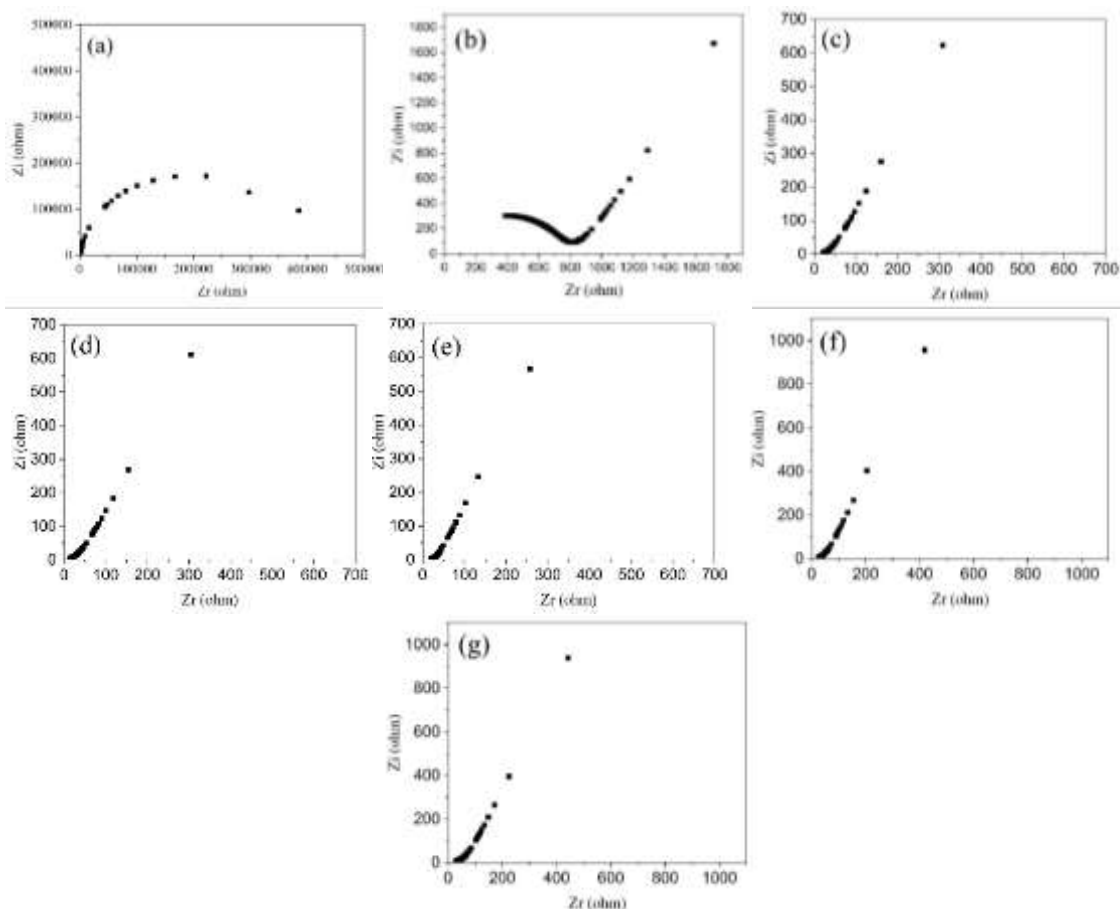


Figure 2. FTIR spectra of pure TSP, TSPL, and TSPL 0.2 – 0.6.

Table 2. Band assignments and shifts in vibrational peaks of plasticized TSP-based electrolyte films.

Pure TSP	TSPL	TSPL 0.2	TSPL 0.3	TSPL 0.4	TSPL 0.5	TSPL 0.6	Spectral band assignments
3340	3375	3394	3391	3381	3371	3371	O–H stretching
2924	2897	2945	2944	2917	2941	2938	CH <sub>2</sub> stretching
1636	1644	1643	1643	1643	1643	1644	C=C stretching
1361	1371	1422	1422	1422	1422	1422	CH <sub>2</sub> bending
-	1265	1248	1249	1249	1250	1251	SO <sub>3</sub> stretching (LiTf)
-	1182	1172	1171	1168	1168	1167	CF <sub>3</sub> stretching (LiTf)
-	-	1074	1074	1074	1074	1074	C–N stretching (DES)
1038	1022	1026	1027	1025	1027	1027	C–O–C stretching
942	944	949	951	948	950	951	C–H bending



**Figure 3.** Cole–Cole plots for (a) pure TSP, (b) TSPL, (c) TSPL 0.2, (d) TSPL 0.3, (e) TSPL 0.4, (f) TSPL 0.5, and (g) TSPL 0.6.

**Table 3.** Ionic conductivity for pure TSP, TSPL, and TSPL 0.2 - 0.6.

Sample Composition	Ionic Conductivity, $\sigma$ (S cm <sup>-1</sup> )
TSP	$4.07 \pm 0.49 \times 10^{-9}$
TSPL	$1.31 \pm 0.01 \times 10^{-5}$
TSPL 0.2	$1.83 \pm 0.12 \times 10^{-4}$
TSPL 0.3	$9.60 \pm 0.04 \times 10^{-5}$
TSPL 0.4	$2.30 \pm 0.21 \times 10^{-4}$
TSPL 0.5	$1.15 \pm 0.14 \times 10^{-4}$
TSPL 0.6	$2.99 \pm 0.13 \times 10^{-5}$

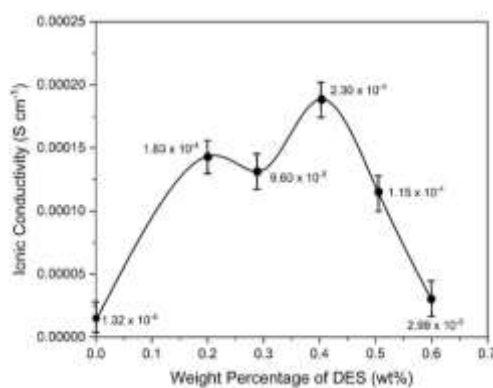


**Figure 4.** Ionic conductivity versus weight percentage of DES (wt%).

Pure TSP film exhibited ionic conductivity of  $4.07 \times 10^{-9} \text{ S cm}^{-1}$ . When LiTf was added, the ionic conductivity increased to  $1.32 \times 10^{-5} \text{ S cm}^{-1}$ . This is due to the presence of charge carrier consisting of  $\text{Li}^+$  ions. The same observation also was reported by Kumar et al. [3], where an increasing ionic conductivity was observed with the addition of salt to pure TSP. When 0.2 wt% of DES was added, the conductivity increased to  $1.83 \times 10^{-4} \text{ S cm}^{-1}$ . This is due to the presence of DES that occupied the space between TSP chains and prevented the formation of hydrogen bonding. This can be supported by the TSP-DES interaction as confirmed from the FTIR analysis. The prevention of hydrogen bonding will suppress the crystallinity of the TSP matrix and provide more amorphous phase to the system, hence facilitating the movement of conducting  $\text{Li}^+$  ions. Apart from that, the presence of free  $\text{Cl}^-$  ions from DES also helped in boosting the ionic conductivity of the system by acting as the transit site for the movement of  $\text{Li}^+$  ions. This can be further confirmed by the salt-DES interaction as observed via the FTIR analysis. The same observation was also reported by Ramesh et al. [17] who studied on the plasticization efficiency of  $\text{ChCl:urea}$  in suppressing the crystallinity of corn starch-based polymer electrolytes.

For TSPL 0.3, the ionic conductivity decreased to  $9.60 \times 10^{-5} \text{ S cm}^{-1}$ . The decline is ascribed to the potential accumulation of additional DES particles creating neutral ion multiples. The presence of neutral ion multiples will obstruct the current conducting pathway. According to this phenomenon, there will be a reduction in the amount of  $\text{Li}^+$  ion transit because of the mobility restriction, hence lowering the ionic conductivity. As 0.4 of wt% of DES was added, the ionic conductivity increased to  $2.30 \times 10^{-4} \text{ S cm}^{-1}$ . This is because the conducting pathway is again created due to dissociation of ion multiples, providing greater availability of amorphous region and additional transit sites that facilitate the mobility of  $\text{Li}^+$  ions. This sample has the potential to be applied in lithium-ion batteries

as its ionic conductivity exceeds the minimum requirement ( $10^{-5} \text{ S cm}^{-1}$ ) of devices [18]. For TSPL 0.5 and TSPL 0.6, the ionic conductivity decreased to  $1.15 \times 10^{-4}$  and  $2.99 \times 10^{-5} \text{ S cm}^{-1}$ , respectively, due to the excessive addition of DES, causing the reformation of ion multiples which obstruct the current conducting pathway. The same observation was also reported by Ramesh et al. [17].

Table 4 presents a comparison of the conductivity observed in our study with that of other polymer electrolyte system incorporating plasticizers. Our findings indicate that the conductivity in our study is generally similar to that of other systems, typically around  $\sim 10^{-4} \text{ S cm}^{-1}$ . It is noteworthy, however, that the conductivity is comparatively lower when contrasted with the research conducted by Maithilee et al. [13], who utilized a non-environmentally friendly plasticizer, EC. On the other hand, Ramesh et al. [17] and Ramesh et al. [19] reported higher conductivity in their PE systems. It is important to note that in their studies, the weight percentage of DES exceeded 50%, resulting in the polymer no longer being the primary component of the system.

#### Morphological Studies

The morphology of the pure TSP film with a rough surface is shown in Figure 5 (a), indicating the presence of a semi-crystalline region in the polysaccharide film. Particle agglomeration was evident in the pure TSP sample, which was probably caused by the hydrogen bond in the polysaccharide maintaining its high crystallinity. This explains the brittleness of the TSP film. The same observation was reported by Wong et al. [23] on the micrograph of pure chitosan. When LiTf was added (Figure 5 (b)), the congested structure was formed, indicating the ion agglomeration due to salt addition. The same observation was reported by Perumal et al. [16] for TSP/magnesium perchlorate ( $\text{Mg}(\text{ClO}_4)_2$ ) system.

**Table 4.** List of ionic conductivities for plasticized polymer electrolyte systems.

Systems	Amount of Plasticizer	Conductivity ( $\text{S cm}^{-1}$ )	References
TSP/LiTf	0.4 wt% $\text{ChCl:1,4-BD}$	$2.30 \times 10^{-4}$	This study
TSP/ sodium nitrite ( $\text{NaNO}_2$ )	0.5 wt% EC	$1.49 \times 10^{-3}$	[13]
Chitosan (CS)/ammonium thiocyanate ( $\text{NH}_4\text{SCN}$ )	40 wt% glycerol	$8.57 \times 10^{-4}$	[20]
CS:methylcellulose (MC)/magnesium acetate ( $\text{Mg}(\text{CH}_3\text{COO})_2$ )/Ni (II)-complex	42 wt% glycerol	$1.02 \times 10^{-4}$	[5]
MC-CH/lithium tetrafluoroborate ( $\text{LiBF}_4$ )	10 wt% PEG	$2.12 \times 10^{-5}$	[21]
Polyurethane acrylate (PUA)/lithium perchlorate ( $\text{LiClO}_4$ )	9 wt% EG	$7.86 \times 10^{-4}$	[22]
CS/lithium bis(trifluoromethanesulfonyl)imide (LiTFSI)	80 wt% $\text{ChCl:Urea}$	$1.04 \times 10^{-3}$	[17]
Cellulose acetate (CA)/LiTFSI	60 wt% $\text{ChCl:Urea}$	$2.61 \times 10^{-3}$	[19]

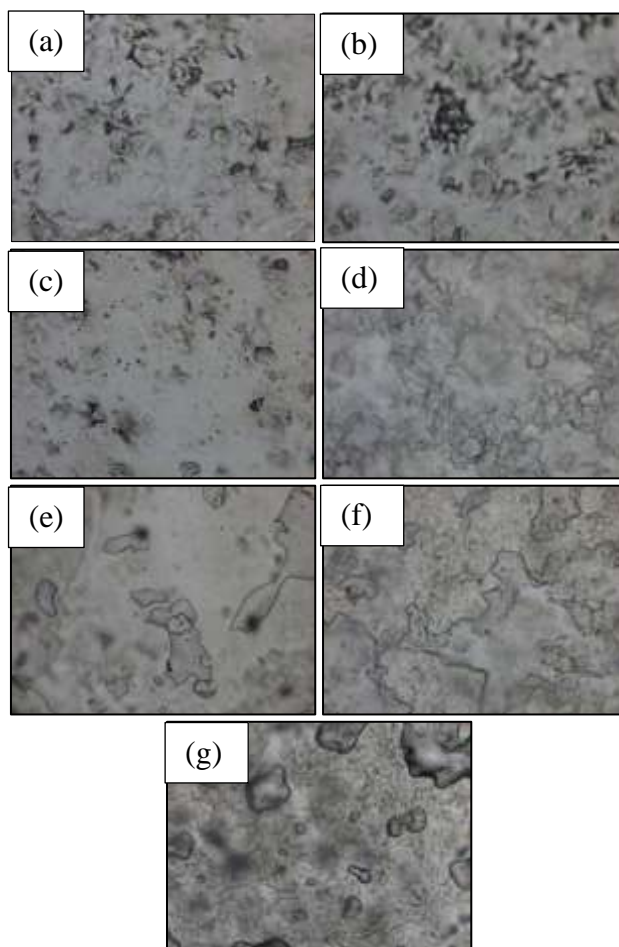


**Figure 5.** Optical micrographs for (a) Pure TSP, (b) TSPL, (c) TSPL 0.2, (d) TSPL 0.3, (e) TSPL 0.4, (f) TSPL 0.5, and (g) TSPL 0.6.

Figures 5 (c)-(g) display the surface morphologies of the electrolyte films after the addition of various weight percentages of DES. For the TSPL 0.2 film, the congested structure seemed to reduce. This might be due to the bulky structure of DES that occupied the space between TSP chains and hindered the formation of hydrogen bonding. Apart from that, the salt-DES interaction, as confirmed from the FTIR analysis, also helped in salt dispersion in the polymer electrolyte. For the TSPL 0.3 film, agglomeration was once again observed. This might be due to the presence of neutral ion multiples due to the accumulation of additional DES particles. This can be further confirmed by the reduction in the conductivity for TSPL 0.3, as observed in the EIS analysis. For the TSPL 0.4 film, agglomeration was reduced. This might be due to the dissociation of ion multiples that cause the agglomeration. This can be further confirmed by the increase in conductivity for TSPL 0.4. For the TSPL 0.5 and 0.6 films, agglomeration was observed again due to the excess amounts of DES which come from

excess ion multiples. This can be further confirmed by the reduced conductivity for both samples. The same observation was reported by Sokolova et al. [24] for chitosan/ChCl-malonic acid system.

#### Mechanical Studies

The films' thickness is a crucial factor in determining their function and goal. A highly thick film has less flexibility, while a thin one is susceptible to fragility and tear easily [25]. Table 5 shows the thickness of the plasticized TSP-based electrolyte films. At  $0.073 \pm 0.02$  mm, the TSPL film is the thinnest if compared to the other compositions. As DES was incorporated, the thickness of the films increased to  $0.108 \pm 0.02$  mm,  $0.120 \pm 0.08$  mm and  $0.122 \pm 0.22$  mm for TSPL 0.2, TSPL 0.4 and TSPL 0.6, respectively. The outcome is consistent with the study of Masdar et al. [25], who reported that the addition of DES had increased the thickness of the pectin films.

**Table 5.** Thickness of TSP films.

Sample Films	Thickness (mm)
TSPL	0.0733 ± 0.02
TSPL0.2	0.1077 ± 0.02
TSPL 0.4	0.1200 ± 0.08
TSPL 0.6	0.1220 ± 0.02

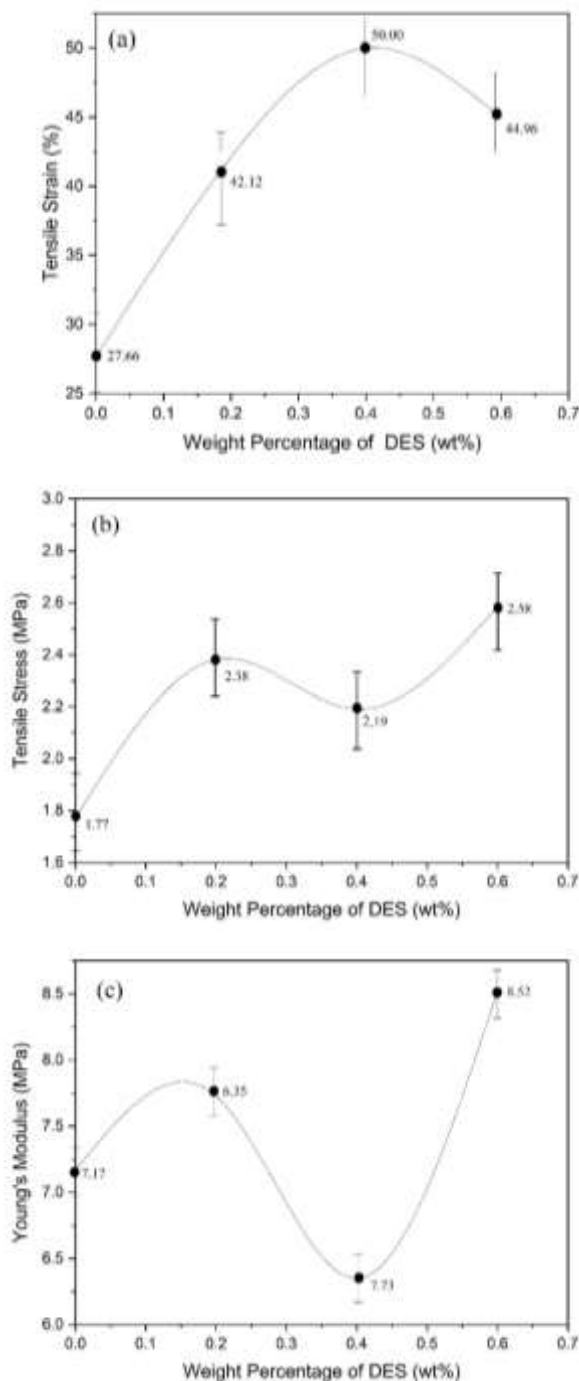


**Figure 6.** Mechanical properties of plasticized TSP-based electrolyte films, (a) tensile stress, (b) tensile strain, and (c) Young's Modulus.

For mechanical testing, ASTM D882 was specifically referred as it is suitable for materials with a thickness of less than one millimeter [26]. Figure 6 (a) shows the tensile strain of the plasticized TSP-based electrolyte films against wt% of DES. When 0.2 and 0.4 wt% of DES were added, the tensile strain increased from 27.66% (TSPL) to 42.12% and 50.00%, respectively. The increase in the tensile strain indicates the improvement in the flexibility of the films and the plasticizing efficiency of the DES. This proves that the incorporated DES had successfully occupied the spaces between TSP chains and hindered the formation of hydrogen bonding, hence forming flexible films. Klongkan et al. [27] stated that adding DOP to a PEO-based polymer electrolyte increases the mobility of the polymer chains by replacing polymer-polymer interactions with polymer-plasticizer interactions. This also helps to lower chain friction and facilitate chain sliding. When 0.6% of DES was added, the tensile strain decreased to 44.96%, indicating the reduced flexibility of the sample. This might be due to the agglomeration of excess DES particles as observed in the OM analyses, which contributes to the brittleness of the film. The same observation was reported by Shamsuri and Daik [28] for agarose/ChCl-urea system.

Figures 6 (b) and (c) show the tensile stress and Young's Modulus of the samples against the wt% of DES. The tensile stress and Young's Modulus display the opposite trend to the tensile strain when different wt% of DES were added, except for the TSPL sample. When 0.2 and 0.4 wt% were added, the tensile stress and Young's Modulus decreased. This is because DES occupied the spaces between TSP chains, which prevents them from getting close to each other and reduces the energy for segmental motion. The same observation was reported by Sirviö et al. [29], which stated that when an effective plasticizer, in this case glycerol, was added the material's resistance to deformation decreased, resulting in a decrease of stiffness and Young's Modulus. When 0.6 wt% of DES was added, the tensile stress and Young's Modulus increased, indicating the highest stiffness of the sample due to the presence of excessive DES particles in it. The same trend was also reported by Shamsuri and Daik [28]. As for the TSPL sample, due to its significantly lower thickness if compared to the other samples, its stiffness was also low.

## CONCLUSION

A flexible and free-standing film of TSP-based polymer electrolyte with improved ionic conductivity of  $2.30 \times 10^{-4} \text{ S cm}^{-1}$  was obtained with the addition of 0.4 wt% of DES. This is due to the presence of DES that occupied the spaces between TSP chains and prevented the formation of hydrogen bonding. The inhibition of hydrogen bonding reduces the crystallinity of the TSP matrix, increasing the amorphous phase within the system, thereby enhancing the mobility of

conducting  $\text{Li}^+$  ions. Additionally, the presence of free  $\text{Cl}^-$  ions from DES further enhanced the system's ionic conductivity by serving as transit sites for  $\text{Li}^+$  ion movement. These statements could be further confirmed by the TSP-DES and salt-DES interactions, as observed via the FTIR analysis. Optical micrographs of TSPL 0.4 revealed a smooth surface devoid of particle agglomeration, indicative of salt-DES interactions, which further contributed to the improved ionic conductivity. Tensile testing demonstrated a maximum tensile strain of 50.00% for TSPL 0.4, affirming its superior flexibility. This system shows promise for application in lithium-ion batteries owing to its favorable ionic conductivity.

## ACKNOWLEDGEMENT

This research was supported by the Ministry of Higher Education through the Fundamental Research Grant Scheme (Grant No. FRGS/1/2023/STG05/UITM/02/19) and Universiti Teknologi MARA.

## REFERENCES

1. Zhu, M., Wu, J., Wang, Y., Song, M., Long, L., Siyal, S. H., Yang, X. & Sui, G. (2019) Recent advances in gel polymer electrolyte for high performance lithium batteries. *Journal of Energy Chemistry*, **37**, 126–142.
2. Bhatia, S. & Bhatia, S. (2016) Natural polymers vs synthetic polymer. *Natural Polymer Drug Delivery Systems: Nanoparticles, Plants, and Algae*, 95–118.
3. Sampath Kumar, L., Christopher Selvin, P. & Selvasekarapandian, S. (2020) Impact of lithium triflate ( $\text{LiCF}_3\text{SO}_3$ ) salt on tamarind seed polysaccharide-based natural solid polymer electrolyte for application in electrochemical device. *Polymer Bulletin*, **78**, 1797–1819.
4. Premalatha, M., Mathavan, T., Selvasekarapandian, S., Monisha, S., Selvalakshmi, S. & Vinoth Pandi, D. (2017) Tamarind seed polysaccharide (TSP)-based Li-ion conducting membranes. *Ionics*, **23**, 2677–2684.
5. Dannoun, E. M., Aziz, S. B., Brza, M. A., M. Nofal M., Asnawi, A. S., Yusof, Y. M. & Woo, H. J. (2020) The study of plasticized solid polymer blend electrolytes based on natural polymers and their application for energy storage EDLC devices. *Polymers*, **12**(11), 2531.
6. Jantrawut, P., Chaiwarit, T., Jantanasakulwong, K., Brachais, C. H. & Chambin, O. (2017) Effect of plasticizer type on tensile property and in vitro indomethacin release of thin films based on low-methoxyl pectin. *Polymers*, **9**(7), 289.

- 176 Muhammad Hanif Mohd Fauzee, Nurul Farah Atieqah Suddin, Nabilah Akemal Muhd Zailani, Khuzaimah Nazir, Sharifah Nafisah Syed Ismail, Nurul Aizan Mohd Zaini, Solhan Yahya and Famiza Abdul Latif
- Impact of Choline Chloride/1,4-Butanediol Deep Eutectic Solvent on Tamarind Seed Polysaccharide-Based Polymer Electrolyte Films
7. Lim, H. & Hoag, S. W. (2013) Plasticizer Effects on Physical–Mechanical Properties of Solvent Cast Soluplus® Films. *Aaps Pharmscitech*, **14**(3), 903–910.
  8. Callaghan, M. A., Alatorre-Hinojosa, S., Connors, L., Singh, R. D. & Thompson, J. L. (2021) Plasticizers and Cardiovascular Health: Role of Adipose Tissue Dysfunction. *Frontiers in Pharmacology*, **11**, 626448.
  9. Paiva, A., Craveiro, R., Aroso, I., Martins, M., Reis, R. L. & Duarte, A. R. C. (2014) Natural deep eutectic solvents—solvents for the 21st century. *ACS Sustainable Chemistry & Engineering*, **2**(5), 1063–1071.
  10. Martins, M. A., Pinho, S. P. & Coutinho, J. A. (2019) Insights into the nature of eutectic and deep eutectic mixtures. *Journal of Solution Chemistry*, **48**, 962–982.
  11. Tomé, L. I., Baião, V., da Silva, W. & Brett, C. M. (2018) Deep eutectic solvents for the production and application of new materials. *Applied Materials Today*, **10**, 30–50.
  12. Shafie, M. H., Yusof, R. & Gan, C. Y. (2019) Synthesis of citric acid monohydrate choline chloride-based Deep Eutectic Solvents (DES) and characterization of their physicochemical properties. *Journal of Molecular Liquids*, **288**, 111081.
  13. Maithilee, K., Sathya, P., Selvasekarapandian, S., Chitra, R. & Meyvel, S. (2023) Investigation on tamarind seed polysaccharide biopolymer electrolyte doped with sodium nitrite and EC plasticizer for primary sodium battery. *Bulletin of Materials Science*, **46**(3), 114.
  14. Nardecchia, S., Gutierrez, M. C., Ferrer, M. L., Alonso, M., Lopez, I. M., Rodríguez-Cabello, J. C. & Del Monte, F. (2012) Phase behavior of elastin-like synthetic recombinamers in deep eutectic solvents. *Biomacromolecules*, **13**(7), 2029–2036.
  15. Latif, F. A., Zailani, N. A. M., Nazir, K., Yusof, R., Ghani, F. S. A., Ishak, M. A. M. & Zamri, S. F. M. (2023) Effect of The Incorporation of Choline Chloride-Based Deep Eutectic Solvent on The Flexibility of Poly (Methyl Methacrylate) Films. *Journal of Sustainability Science and Management*, **18**(12), 28–42.
  16. Perumal, P., Abhilash, K. P., Sivaraj, P. & Selvin, P. C. (2019) Study on Mg-ion conducting solid biopolymer electrolytes based on tamarind seed polysaccharide for magnesium ion batteries. *Materials Research Bulletin*, **118**, 110490.
  17. Ramesh, S., Shanti, R. & Morris, E. (2012) Studies on the plasticization efficiency of deep eutectic solvent in suppressing the crystallinity of corn starch-based polymer electrolytes. *Carbohydrate polymers*, **87**(1), 701–706.
  18. Yue, L., Ma, J., Zhang, J., Zhao, J., Dong, S., Liu, Z. & Chen, L. (2016) All solid-state polymer electrolytes for high-performance lithium ion batteries. *Energy Storage Materials*, **5**, 139–164.
  19. Ramesh, S., Yin, T. S. & Liew, C. W. (2011) Effect of dibutyl phthalate as plasticizer on high-molecular weight poly (vinyl chloride)–lithium tetraborate-based solid polymer electrolytes. *Ionics*, **17**, 705–713.
  20. Aziz, S. B., Nofal, M. M., Abdulwahid, R. T., Kadir, M. F. Z., Hadi, J. M., Hessien, M. M. & Saeed, S. R. (2021) Impedance, FTIR and transport properties of plasticized proton conducting biopolymer electrolyte based on chitosan for electrochemical device application. *Results in Physics*, **29**, 104770.
  21. Ahmed, H. T., Jalal, V. J., Tahir, D. A., Mohamad, A. H. & Abdullah, O. G. (2019) Effect of PEG as a plasticizer on the electrical and optical properties of polymer blend electrolyte MC-CH-LiBF<sub>4</sub> based films. *Results in Physics*, **15**, 102735.
  22. Tuan Naiwi, T. S. R., Aung, M. M., Ahmad, A., Rayung, M., Su'ait, M. S., Yusof, N. A. & Wynn Lae, K. Z. (2018) Enhancement of plasticizing effect on bio-based polyurethane acrylate solid polymer electrolyte and its properties. *Polymers*, **10**(10), 1142.
  23. Wong, W. Y., Wong, C. Y., Walvekar, R. & Khalid, M. (2018) Choline chloride: Urea-based deep eutectic solvent as additive to proton conducting chitosan films. *Journal of Engineering Science and Technology*, **13**(2), 2995–3006.
  24. Sokolova, M. P., Smirnov, M. A., Samarov, A. A., Bobrova, N. V., Vorobiov, V. K., Popova, E. N. & Toikka, A. M. (2018) Plasticizing of chitosan films with deep eutectic mixture of malonic acid and choline chloride. *Carbohydrate Polymers*, **197**, 548–557.
  25. Masdar, N. D., Yusof, R. & Ramzani, N. A. (2022) Effect of deep eutectic solvent on tensile properties and biodegradation of pectin with eggshell bioplastic. *Malaysian Journal of Analytical Sciences*, **26**(1), 58–69.
  26. Raj, S. S., Kuzmin, A. M., Subramanian, K., Sathiamoorthy, S. & Kandasamy, K. T. (2021) Philosophy of selecting ASTM standards for mechanical characterization of polymers and

- polymer composites. *Materiale Plastica*, **58(3)**, 247–256.
27. Klongkan, S. & Pumchusak, J. (2015) Effects of nano alumina and plasticizers on morphology, ionic conductivity, thermal and mechanical properties of PEO-LiCF<sub>3</sub>SO<sub>3</sub> solid polymer electrolyte. *Electrochimica Acta*, **161**, 171–176.
28. Shamsuri, A. A. & Daik, R. (2012) Plasticizing effect of choline chloride/urea eutectic-based ionic liquid on physicochemical properties of agarose films. *BioResources*, **7(4)**.
29. Sirviö, J. A., Visanko, M., Ukkola, J. & Liimatainen, H. (2018) Effect of plasticizers on the mechanical and thermomechanical properties of cellulose-based biocomposite films. *Industrial Crops and Products*, **122**, 513–521.